A New Approach to the Study of Transient Protein Conformations: The Formation of a Semiburied Salt Link in the Folding Pathway of Barnase

Mikael Oliveberg and Alan R. Fersht*

Cambridge Centre for Protein Engineering, Hills Road, Cambridge CB2 2QH, England

Received December 12, 1995; Revised Manuscript Received March 18, 1996[⊗]

ABSTRACT: We use in this study a novel kinetic approach to determine the H^+ titration properties of a semiburied salt link in the transition state for unfolding of barnase. The approach is based on changes in the pH dependence of the kinetics upon mutation of a target residue. This makes it relatively insensitive to the absolute value of the stability and, thereby, to artifacts caused by structural rearrangements around the site of mutation. The semiburied salt bridge studied here is between Asp93 and Arg69. Mutation of either residue significantly destabilizes the protein, and the pK_a value of Asp93 is severely lowered in the native state to below 1 because of the ionic interaction with Arg69. The Asp93−Arg69 salt link appears to be formed early in the folding process; the pK_a value of Asp93 in the transition state (∼1) is similar to that in the native state, and deletion of the ionic interaction with Arg69 substantially destabilizes the folding intermediate and changes the kinetic behavior from multistate to two-state or close to two-state, depending on the conditions. The results suggest that the formation of ionic interactions within clusters of hydrophobic residues can be important for early folding events and can control kinetically the folding pathway. This is not because of the inherent stability of the salt link but because the presence of two unpaired charges is very unfavorable. The data reveal also that fractional Φ values are consistent with a uniformly expanded transition state or one with closely spaced energy levels and not with parallel folding pathways.

The complete description of a protein-folding pathway requires characterization of all ground states, high-energy intermediates, and transition states. Whereas ground states of proteins (i.e., native conformations and various denatured states) can be isolated and studied directly under equilibrium conditions, the properties of high-energy intermediates and transition states can only be studied indirectly by kinetic methods. The coupling between reaction rates and the energetics of activation barriers, or transition states, was first described by Arrhenius in 1889 (Arrhenius, 1889) and was later given a quantum-mechanical formulation by Eyring in the transition state theory (Eyring, 1935) (eq 1, below). The original formulation of transition state theory assumes that the reaction rate at any temperature depends only on the concentration of the activated complex and that the rate constant of crossover for this activated species is limited by the vibrational frequency of the atoms ($k_BT/h \approx 10^{13}$ s^{-1}). In protein-folding processes, however, the activation barriers are not localized elementary steps but involve a high dimensionality because of the cooperative rearrangements of multiple amino acid residues and solvent molecules. Accordingly, the rate of crossover may well be different (slower) than the vibrational frequency of individual atoms, and it is not possible to verify the physical reality of the parameters determined by the transition state theory. The problem may be partly overcome by focusing on the ground state and the transition state being in quasi-thermodynamic equilibrium (Fersht *et al.*, 1992; Oliveberg *et al.*, 1995b). In this equilibrium, it can be argued that the temperature and solvent dependence of the rate constants should be similar to that of the equilibrium constant; i.e., the rate of crossover of the activated complex is approximately constant. Along these lines, it is possible to evaluate *changes* in the quasi-thermodynamic free energy of activation ($\Delta G^{\ddagger}$), although the significance of its absolute value is unclear. Such changes in $\Delta G^{\ddagger}$ can be induced by solvent (Oliveberg & Fersht, 1996a), by temperature (Pohl, 1976; Sugihara & Segawa, 1984; Chen *et al.*, 1989; Oliveberg & Fersht, 1996b), as well as by chemical or mutational modification of the protein itself (Matouschek *et al.*, 1989).

The thermodynamic properties of the transition state for unfolding can be monitored directly by the unfolding rate constant (k_u) since this corresponds to the free energy difference between the native protein and the transition state, i.e., the high-energy barrier that constitutes the rate-limiting step for the unfolding reaction. The parameters derived from the refolding reaction, on the other hand, are more difficult to interpret; the observed refolding rate constant (k_f^{obs}) is determined not only by the activation free energy for the refolding process but also by variations in the kinetic pre-equilibrium, i.e., the extent of accumulation of folding intermediates (Oliveberg & Fersht, 1996a,b; Oliveberg *et al.*, 1995b). Experimental observations of the unfolding kinetics suggest that the transition state for unfolding is a compact dehydrated conformation close to the native state on the reaction coordinate (Sugihara & Segawa, 1984; Oliveberg & Fersht, 1996a,b). A detailed description of transition states on the level of individual interactions has been provided by an extensive mutational and thermodynamic approach for barnase (Matouschek *et al.*, 1989; Serrano *et al.*, 1992; Fersht, 1993) and for chymotrypsin inhibitor 2 (CI2) (Otzen *et al.*, 1994; Itzhaki *et al.*, 1995). In these studies, the interaction energies between individual residues and the rest of the protein are used as structural probes, and the

* To whom correspondence should be addressed.

[⊗] Abstract published in *Advance ACS Abstracts,* May 1, 1996.

S0006-2960(95)02931-X CCC: $12.00

destabilization of the transition state upon mutation of a target residue is used to quantify the extent of interaction in the transition state. Taken together, the data suggest that peripheral parts of the proteins are loosened up in the transition state whereas the centers of hydrophobic cores and some elements of secondary structure remain relatively intact. However, there is an important difference between barnase and CI2; barnase, which appears to refold via the accumulation of a transient intermediate, shows a higher structural content in the transition state than does CI2 which refolds without the accumulation of a transient intermediate. A consistent picture is given by the heat capacity of the transition states; the hydration of the transition state of barnase is close to that of the native state (Oliveberg & Fersht, 1996b), whereas the hydration of the transition state of CI2 is intermediate between the native and the denatured conformations (Jackson & Fersht, 1991).

An uncertainty when using free energy effects of truncated residues as probes for structural content is possible reorganizations of the mutant protein (Tissot *et al.*, 1996). Reorganization of the structure around the site of mutation might counteract the stability loss and, thereby, complicate the observed interaction energy of the truncated moiety. The structural response to cavity-creating mutations in hydrophobic cores involves relatively small movements of atoms around the truncated residue (Eriksson *et al.*, 1992; Buckle *et al.*, 1993; Jackson *et al.*, 1993). The problem is whether this can be assumed also for transition states and folding intermediates since these are likely to be significantly expanded and, hence, less rigid than the native protein.

To test the results from previous mutant studies, we report here a new approach to obtain interaction energies in the transition state. The approach is exemplified in the unfolding reaction of the small ribonuclease barnase (EC 3.1.27.3). We utilize the change in pH dependence of the activation energy upon mutation of a carboxylate group (Asp93) which is involved in a strong salt bridge with Arg69. For comparison, this salt bridge is analyzed also by conventional methods in the accompanying paper (Tissot *et al.*, 1996). Whereas previous studies rely on the *magnitude* of the change of the activation energy upon mutation ($\Delta\Delta G^{\ddagger}$), this study relies on changes of $\Delta\Delta G^{\ddagger}$ with pH, i.e., $\partial\Delta\Delta G^{\ddagger}/\partial$pH. The advantage of this method is that the pH dependence of the activation energy can be considered independent of reorganization effects since these will contribute only to an offset of $\Delta\Delta G^{\ddagger}$ and, therefore, do not affect $\partial\Delta\Delta G^{\ddagger}/\partial$pH. With the double mutant approach, these effects can only be accounted for if $\Delta\Delta G^{\ddagger}$ and the stability change of the native state are altered by the same extent by the reorganization (Tissot *et al.*, 1996). Our results regarding the formation of the Asp93−Arg69 salt bridge in the transition state of barnase are in good agreement with those obtained by stability changes ($\Delta\Delta G^{\ddagger}$) at pH 6.3 in the accompanying paper (Tissot *et al.*, 1996). We provide further the dependence on pH and ionic strength of this ionic interaction, which reflects the titration properties and the pK_a value for Asp93 in the transition state as well as in the native protein.

MATERIALS AND METHODS

Materials. Barnase was overexpressed and purified from *Escherichia coli* as described in Serrano and Fersht (1989). Site-directed mutagenesis was done by standard procedures (Sayers *et al.*, 1988) using a kit from Amersham. The buffers used were 50 mM glycine and HCl (pH 1.5−3.0), 50 mM sodium formate/formic acid (pH 2.7−4.2), 50 mM sodium acetate/acetic acid (pH 3.7−5.3), and 50 mM 2-(*N*-morpholino)ethanesulfonic acid (MES) (pH 6.3). HCl/KCl was used between pH 1.5 and 0.2. The ionic strength (μ) was controlled with KCl. All chemicals were of analytical grade and were purchased from Sigma.

Stopped-Flow Experiments. The unfolding and refolding processes of barnase were induced by rapid mixing of the protein into various buffers in order to achieve a rapid change in pH. The instrument used was an Applied Photophysics DX-17 MV stopped-flow spectrofluorimeter connected to a Grant LTD 6 thermostatted water bath. The thermostatting system maintained the temperature of the reservoir syringes and the observation cell within ±0.1 °C. The stopped-flow instrument was set up to mix the protein solution with unfolding and refolding buffer solutions in a volumetric ratio of 1:1, yielding a final protein concentration of 8 μM and a final buffer concentration of 50 mM. The kinetics was monitored by fluorescence changes. Excitation was at 280 nm and the emission collected at wavelengths greater than 315 or 335 nm, using cutoff filters. For studies of the pH dependence of the unfolding kinetics [k_u(pH)], the native protein was first dissolved in pure water and then mixed with acidic buffers into denaturing conditions, typically in the range of pH 3−0.2. For studies of the pH dependence of the observed refolding kinetics [k_f^{obs}(pH)], the protein was first dissolved and left to denature in 32 mM HCl (pH 1.5). The acid-denatured protein was subsequently mixed with buffers into refolding conditions at higher pH values, typically between pH 2 and 6.3. To maintain the ionic strength constant at 50 or 600 mM, KCl was included in the syringes containing the refolding/unfolding buffer. This avoids any perturbation of the initial state of the protein, i.e., polymerization or aggregation processes (Oliveberg & Fersht, 1996a).

Data Analysis. The rate constants and amplitudes of the folding reactions were obtained by fitting a sum of exponential functions to the acquired data, using the data analysis program Kaleidagraph (Adelbeck Software). In some cases, a linear slope was included in the exponential expression to account for machine drift or photolysis caused by the excitation light. When the results were mathematically processed, i.e., a series of closely spaced data points versus pH, a "smooth function" (Kaleidagraph) was fitted to the data, and this smooth function was then used to represent mathematically the experimental values.

Extrapolation of Stopped-Flow Data Obtained at High Temperatures to 25 °C. The unfolding kinetics at 25 °C cannot be studied directly by mixing experiments under conditions where only the native state is populated. Therefore, we have earlier adopted an approach where the unfolding experiments are carried out at high temperatures. At these temperatures, the midpoint for the unfolding transition of the mutant protein occurs above pH 4 and, hence, the denatured state is the predominant species at lower pH values, which enables the unfolding kinetics to be followed from about pH 3.5 and downward (Oliveberg & Fersht, 1996a). The unfolding rate constants obtained from the high-temperature experiments, however, have to be

extrapolated to 25 °C using the temperature dependence of the unfolding rate constant. The temperature dependence of k_u(pH) is described by the transition state theory

$$\ln\left[\frac{k_u(\mathrm{pH})}{T}\right] = \ln\left(\frac{k_B}{h}\right) - \frac{\Delta G^{\ddagger}(\mathrm{pH})}{RT} = \ln\left(\frac{k_B}{h}\right) + \frac{\Delta S^{\ddagger}(\mathrm{pH})}{R} - \frac{\Delta H^{\ddagger}(\mathrm{pH})}{RT} \quad (1)$$

where k_B is Boltzmann's constant, h is Planck's constant, T is the absolute temperature, R is the gas constant, and $\Delta G^{\ddagger}$(pH), $\Delta H^{\ddagger}$(pH), and $\Delta S^{\ddagger}$(pH) are the (pH dependent) free energy of activation, activation enthalpy, and activation entropy, respectively. The value of $\Delta H^{\ddagger}$(pH) at each pH was obtained from the slope of the corresponding Eyring plots [$\ln(k_u/T)$ versus $1/T$] (Figure 2). The values of $\Delta H^{\ddagger}$(pH) were subsequently plotted versus pH, and a linear function [$\Delta H^{\ddagger}$(pH) = $\alpha + \beta$(pH)] was fitted to the plot (Figure 2) and used in eq 2 below. To obtain an expression suitable for the extrapolation of k_u(pH) from any temperature (T) to 298.15 K (25.00 °C), eq 1 was divided with the corresponding expression for k_u(pH) at $T = 298.15$ K, which gives

$$\log k_u^{298.15}(\mathrm{pH}) = \log k_u^{T}(\mathrm{pH}) - {}^{1}/_{2.3}\left[(\alpha + \beta(\mathrm{pH}))\left(\frac{1}{T} - \frac{1}{298.15}\right) - \ln\left(\frac{298.15}{T}\right)\right] \quad (2)$$

where $\alpha + \beta$(pH) = $\Delta H^{\ddagger}$(pH), obtained from the plot in Figure 2. It is assumed in eqs 1 and 2 that $\Delta H^{\ddagger}$ and $\Delta S^{\ddagger}$ are independent of temperature which in turn relies on a negligible change in heat capacity (ΔC_p) between the native protein and the transition state. The dependence of $\ln(k_u/T)$ on $1/T$ will then become linear, consistent with the experimental behavior of the unfolding kinetics [Figure 2; see also Oliveberg and Fersht (1996b)].

Relationship between the pH Dependence of $\Delta G_{A/B}$ and the Difference in the Degree of Protonation of the Protein States A and B. It can be shown from the law of mass action that the difference in the number of bound protons between two protein conformations, A and B, is related to the pH dependence of the free energy difference between these conformations (Tanford, 1970):

$$\frac{\partial[\Delta G_{A-B}(\mathrm{pH})]}{\partial(\mathrm{pH})} = 2.3RT[Q_A(\mathrm{pH}) - Q_B(\mathrm{pH})] = 2.3RT\Delta Q_{A-B}(\mathrm{pH}) \quad (3)$$

where ΔG_{A-B} is the difference in free energy between state A and B. Q_A(pH) and Q_B(pH) are the number of protons bound to state A and B, respectively, and ΔQ_{A-B}(pH) is the change in the number of protons released on the transition from A to B.

The first order rate constant for the unfolding process [k_u(pH)] is related to the free energy difference between the native state and the major transition state according to eq 1. Hence, the observed pH dependence of log k_u(pH) is directly proportional to the pH dependence of $\Delta G^{\ddagger}$(pH) = $\Delta H^{\ddagger}$(pH) + $T\Delta S^{\ddagger}$(pH) and can be related to $\Delta Q_{\ddagger-N}$(pH) according to

$$\frac{\partial \log k_u}{\partial pH} = -\frac{1}{2.3RT}\frac{\partial \Delta G^{\ddagger}}{\partial pH} = -\Delta Q_{\ddagger-N}(\mathrm{pH}) \quad (4)$$

Equation 4 applies also to the refolding rate constant but will, in this case, yield the change in ionization between the denatured ground state and the transition state, $\Delta Q_{\ddagger-D}$(pH).

RESULTS

The strategy for probing the Asp93−Arg69 salt bridge is based on the pK_a value of the carboxylate group of Asp93. This is determined by comparing the pH dependence of the stability of wild-type and mutant protein. The pH dependence of the stability of the native state is measured directly by thermal unfolding at equilibrium, whereas the pH dependence of the stability of the folding intermediate and the transition state is determined by stopped-flow kinetics.

Nomenclature for the Rate Constants

The rate constants that are obtained directly from experimental time courses are referred to as the observed rate constants (k^{obs}). These can be either observed refolding rate constants (k_f^{obs}) or observed unfolding rate constants (k_u^{obs}). These observed rate constants, however, do not always correspond to the true refolding and unfolding rate constants (k_f and k_u) (see eq 5 below).

pH Dependence of the Unfolding and Refolding Kinetics Observed at 25 °C

The unfolding of wild-type barnase and the Asp93 → Asn mutant shows an overall decrease in fluorescence, whereas the refolding reaction shows an increase in fluorescence. The time course of the unfolding process is seen as a major exponential decay in fluorescence. Under conditions where the final state is a mixture of native and denatured conformations, the major unfolding phase is followed by slow first order re-equilibration caused by *trans* to *cis* isomerizations around the peptidyl proline bonds in the denatured state [data not shown; see Oliveberg *et al.* (1995a)]. The pH dependence of the unfolding rate constant for wild-type barnase and the Asp93 → Asn mutant at 25 °C is shown in the top panels of Figure 1. The unfolding rate constant (k_u) increases progressively at lower pH values, and its pH dependence is more pronounced at $\mu = 50$ mM than at $\mu = 600$ mM. At $\mu = 50$ mM, the mutant protein unfolds faster than the wild type, but at $\mu = 600$ mM, the unfolding rate constants are similar (Figure 1). The amplitude of the unfolding time course decreases rapidly around the pH for the transition midpoint. This occurs because the change in fluorescence is directly related to the proportion of unfolded protein at the final conditions of the stopped-flow experiment. The pH for the transition midpoint for the Asp93 → Asn mutant at 25 °C is ~2.7 at $\mu = 50$ mM and ~1.8 at $\mu = 600$ mM (Oliveberg *et al.*, 1995a) (cf. Figure 4).

The top panels in Figure 1 also show the pH dependence of the refolding rate constant for wild-type barnase and the Asp93 → Asn mutant at 25 °C. In contrast to the unfolding reaction, the rate constant for refolding (k_f^{obs}) is observed to increase with pH under acidic conditions. The pH dependence of log k_f^{obs} levels off around pH 4, and the rate constant shows a maximum around pH 5. Hence, k_f^{obs} is slightly lower at standard conditions at pH 6.3 than at pH 4−5. Under all conditions, the refolding rate constant for wild-type barnase is faster than that for the Asp93 → Asn mutant. The amplitude for the refolding reaction increases rapidly around the pH for the transition midpoint (Figure

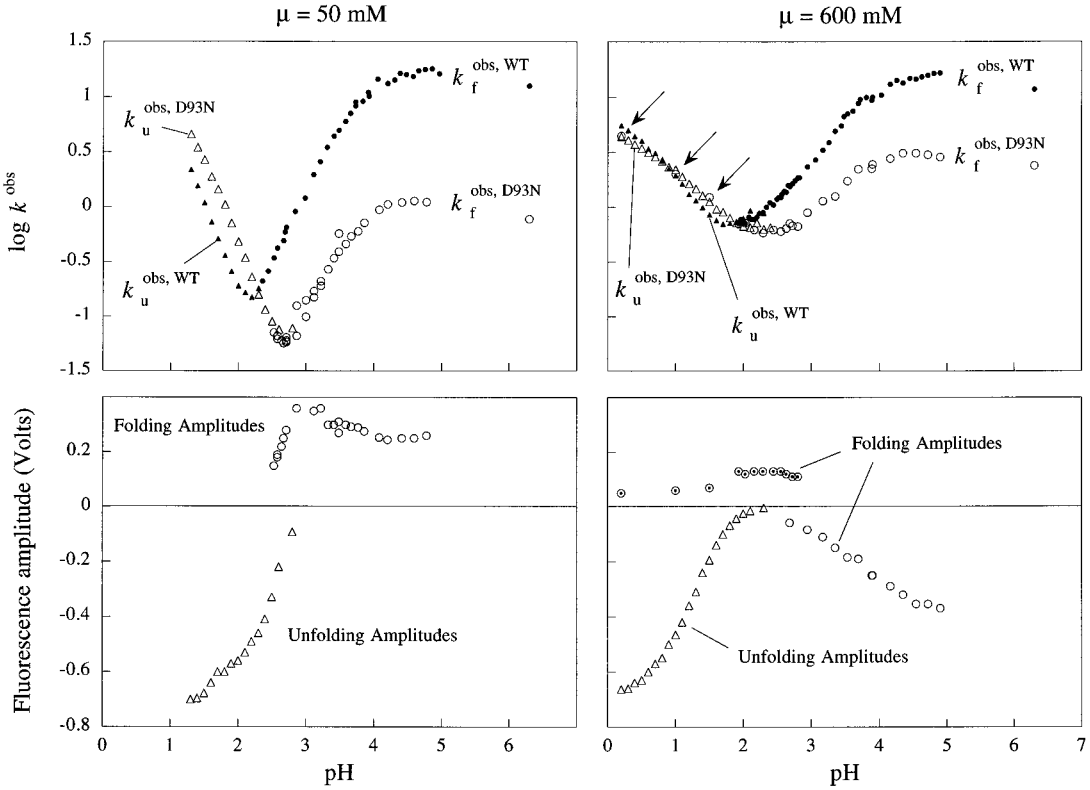

FIGURE 1: pH dependence of the unfolding and refolding kinetics of wild-type barnase and the Asp93 → Asn mutant, as observed at 25 °C. k has units of s^{-1}. The data were collected using a 315 nm cutoff filter unless otherwise stated. (Top left panel) Data obtained at a constant ionic strength of 50 mM: (▲) the observed unfolding rate constant for wild-type protein ($k_u^{obs,WT}$), (△) the unfolding rate constant for the Asp93 → Asn mutant ($k_u^{obs,D93N}$), (●) the observed refolding rate constant for wild-type protein ($k_f^{obs,WT}$), and (○) the refolding rate constant for the Asp93 → Asn mutant ($k_f^{obs,D93N}$). (Top right panel) The corresponding data obtained at a constant ionic strength of 600 mM. The arrows indicate the rate constant of the refolding process for the Asp93 → Asn mutant that can be detected also at pH values well below the transition midpoint. This shows that the mutant protein does not unfold completely with pH so that a small fraction of the native protein is still present at pH 0.2. Under conditions where both the native and denatured protein are populated, k_u^{obs} and k_f^{obs} show the same value since the observed rate constant is always the sum of the forward and reverse rate constants (eq 5). (Bottom left panel) $\mu = 50$ mM: (△) the change in fluorescence upon unfolding of the Asp93 → Asn mutant and (○) the change upon refolding of the Asp93 → Asn mutant. (Bottom right panel) $\mu = 600$ mM: (△) the unfolding amplitude of the Asp93 → Asn mutant. The corresponding refolding amplitudes (⊙) using a 335 nm cutoff filter and (○) using a 315 nm cuoff filter.

1). With the Asp93 → Asn mutant, the denaturation with acid is incomplete at $\mu = 600$ mM and the refolding process is observed throughout the experimental pH range (mixing protein denatured in 32 mM HCl with high-salt buffers). Below the transition midpoint, however, the rate constant observed for the (fractional) refolding reaction follows precisely that for the unfolding reaction (arrows in Figure 1). This behavior is predicted since, at all conditions, the observed rate constant (k^{obs}) is the sum of the unfolding and refolding rate constants,

$$k^{obs} = k_f + k_u \qquad (5)$$

so that $k^{obs} \approx k_u$ under denaturing conditions where $k_f < k_u$, and $k^{obs} \approx k_f$ under stabilizing conditions where $k_f > k_u$. Hence, the observed refolding reaction is dominated by k_u at pH values below the transition midpoint, and *vice versa*, the curvature observed for the unfolding kinetics in the transition region is due to an increased contribution from the refolding rate constant (Figure 1).

Temperature Dependence of the Unfolding Kinetics at Different pH Values

The temperature dependence of the observed unfolding rate constant (k_u^{obs}) for the Asp93 → Asn mutant is shown in the Eyring plot in Figure 2. At a given temperature, the unfolding rate constant is higher at lower pH values (cf. Figure 1). At most pH values, the Eyring plots are linear, indicating a negligible change in heat capacity between the denatured state and the transition state for unfolding. This is consistent with the behavior observed for the wild-type protein (Oliveberg & Fersht, 1996a). At the highest pH value, however, $\ln(k_u^{obs}/T)$ versus $1/T$ displays an upward curvature at lower temperatures which is induced by the influence of the refolding rate constant as the temperature becomes close to the temperature for the transition midpoint (eq 5). The activation enthalpies ($\Delta H^{\ddagger}$) which are obtained from the Eyring plots according to eq 1 are plotted versus pH in the bottom panel of Figure 2. The activation enthalpy of the Asp93 → Asn mutant is about 5 kcal/mol lower than that observed for the wild-type protein, although the pH dependence of $\Delta H^{\ddagger}$ appears unaffected by the mutation. Linear functions fitted to the data yield $\Delta H^{\ddagger,WT}(pH) = 30\,030\ (\pm 490) + 3779\ (\pm 240) \times pH$ and $\Delta H^{\ddagger,Asn93}(pH = 24\,290\ (\pm 204) + 4105\ (\pm 105) \times pH$. $\Delta H^{\ddagger}$ shows no significant dependence on ionic strength.

Extrapolation of High-Temperature Unfolding Data to 25 °C

In order to obtain information about k_u at 25 °C and at pH values where the observed rate constant is dominated

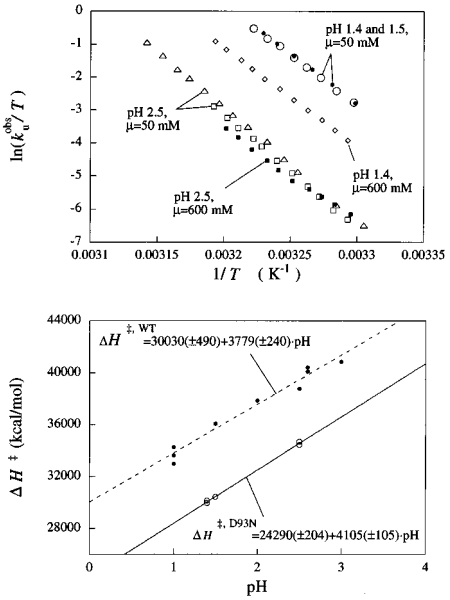

FIGURE 2: Temperature dependence of the unfolding rate constant as a function of pH. k/T has units of s^{-1} K^{-1}. (Top panel) The temperature dependence of the unfolding rate constant for the Asp93 → Asn mutant at pH 2.5 and $\mu = 50$ mM (△, □), pH 2.5 and $\mu = 600$ mM (■), pH 1.5 and $\mu = 50$ mM (○), pH 1.4 and $\mu = 50$ mM (●), and pH 1.4 and $\mu = 600$ mM (◇). The activation enthalpy ($\Delta H^{\ddagger}$) is obtained from the slope of these plots according to eq 1. The data set obtained at pH 2.5 and $\mu = 600$ mM (■) is not used in the calculations since part of the observed kinetics in this case is affected by the refolding rate constant (see text). (Bottom panel) The pH dependence of the activation enthalpy of the unfolding rate constant for wild-type barnase (●) and the Asp93 → Asn mutant (○). Linear functions are fitted to the plots, and these functions are used to represent $\Delta H^{\ddagger}$(pH) in the extrapolation of high-temperature unfolding data to 25 °C (eq 2).

by k_f (i.e., above pH 2, Figure 1), acid-unfolding experiments were performed at a set of higher temperatures and extrapolated to 25 °C according to eq 2; at these elevated temperatures, the protein is found substantially destabilized and, hence, the observed unfolding rate constant (k_u^{obs}) is dominated by k_u (eq 5). The pH dependence of the unfolding kinetics for the Asp93 → Asn mutant at 25, 35, 42, and 44.1 °C is shown in the top panels of Figure 3. The temperatures and the range of pH values used are chosen so that the influence of the refolding rate constant on the kinetics is negligible. The bottom panels of Figure 3 show the unfolding data extrapolated to 25 °C, using the activation enthalpies from Figure 2 (eq 2). Although the way of determining k_u at 25 °C at first may appear susceptible to considerable errors, the precise overlap of rate constants extrapolated from different temperatures reveals the high accuracy of the kinetic data and the extrapolation procedure (Figure 3).

Deviations between the Observed Unfolding Rate Constant and That Extrapolated from 35 °C Reveal the Protein Stability at Low pH Values

It has been demonstrated previously by thermal unfolding experiments that the pH dependence of the stability of barnase increases significantly at low pH at $\mu = 600$ mM and that the stabilities observed under these conditions suggest incomplete unfolding (Oliveberg *et al.*, 1994, 1995a). To test independently these results, we now compare the unfolding rate constant which has been extrapolated from 35 to 25 °C with that observed for the unfolding reaction at 25 °C (top panels, Figure 4); the extrapolated rate constant is assumed to represent k_u, whereas the observed rate constant will contain contributions from both k_u and k_f if the protein is not completely unfolded (eq 5). Conveniently, barnase and its mutants are observed to display a two-state unfolding reaction under destabilizing conditions. As a working model, we assume that the two-state behavior extends also into unfolding conditions; according to a two-state model and eq 5,

$$K_{D-N} = k_u/k_f \Rightarrow \log(k_u + k_f) - \log(k_u) = \log(1 + 1/K_{D-N}) \quad (6)$$

where K_{D-N} is the equilibrium constant for unfolding. The stability (or free energy of unfolding) is then easily calculated from K_{D-N} by the thermodynamic identity $\Delta G_{D-N} = -2.3RT \log(K_{D-N})$. The free energy of unfolding was calculated from the kinetic data in Figure 4 (eq 6) and compared with stability data from thermal unfolding experiments for wild-type barnase and the Asp93 → Asn mutant. As seen in the bottom panels of Figure 4, the kinetic data are in remarkably good agreement with the equilibrium experiments. The result confirms that (i) barnase displays two-state behavior at unfolding conditions (Oliveberg & Fersht, 1996a,b), and (ii) the thermal denaturation data at $\mu = 600$ mM are reliable and are not perturbed by aggregation of the unfolded state [see Oliveberg *et al.* (1994) and Oliveberg and Fersht (1996b)].

Characterization of the Transition State for Unfolding

(1) Difference in the Degree of Protonation between N and ‡. The pH dependence of the unfolding rate constant (k_u) is related to the ionization difference between the native state and the transition state for unfolding ($\Delta Q_{N-\ddagger}$) according to eq 4. To obtain the gradient of log k_u versus pH ($\partial \log k_u/\partial$pH), a third order polynomial function was fitted to the unfolding rate constants for wild-type and mutant protein (top panels, Figure 5), and the derivative of this function is used to represent $\Delta Q_{\ddagger-N}$(pH) (bottom panels, Figure 5). At $\mu = 50$ mM, both wild-type and mutant proteins show a value of $\Delta Q_{\ddagger-N} \approx 1.7$ between pH 3.5 and 2. Below pH 2, the pH dependence of the Asp93 → Asn mutant decreases more rapidly than is observed for the wild-type protein so that at pH 1.3 the difference between $\Delta Q_{\ddagger-N}^{WT}$ and $\Delta Q_{\ddagger-N}^{Asn93}$ is approximately 0.6 (left bottom panel, Figure 5). At $\mu = 600$ mM, the values of $\Delta Q_{\ddagger-N}^{WT}$ and $\Delta Q_{\ddagger-N}^{Asn93}$ diverge already below pH 3. The resulting difference (about 0.2) remains constant down to pH 1.5 where $\Delta Q_{\ddagger-N}^{WT}$ and $\Delta Q_{\ddagger-N}^{Asn93}$ appear to converge at a value of 0.5 (right bottom panel, Figure 5).

Polynomial fits give a restricted but clearer estimate of the derivative in cases with a large number of scattered data points than do the "smoothed" functions which have been used for the analysis of thermal stability data [cf. Oliveberg *et al.* (1994)]. With the unfolding rate constants, the derivative obtained from a smooth function is scattered symmetrically around the values obtained from the polynomial fit and, hence, the two procedures yield consistent results (data not shown).

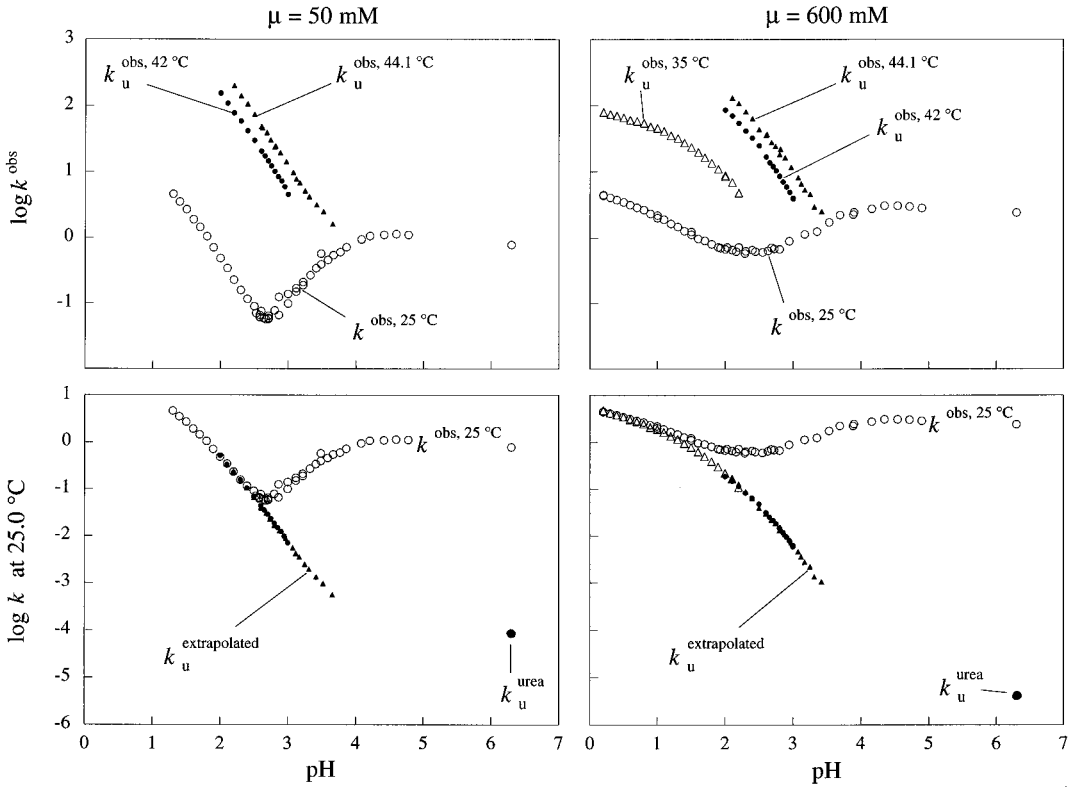

FIGURE 3: pH dependence of the unfolding rate constant for the Asp93 → Asn mutant of barnase at high temperatures and extrapolated to 25 °C (○). k has units of s^{-1}. (Top left panel) $\mu = 50$ mM. The unfolding rate constant at 42 °C (●) and 44.1 °C (▲) in comparison with the kinetics observed at 25 °C. (Top right panel) $\mu = 600$ mM. The unfolding rate constant at 42 °C (●), 44.1 °C (▲) and 35 °C (△) in comparison with the kinetics observed at 25 °C (○). (Bottom left panel) $\mu = 50$ mM. The pH dependence of the unfolding rate constant at 25 °C as obtained from high-temperature data according to eq 2) ($k_u^{extrapolated}$), in comparison with the kinetics observed at 25 °C (○). (Bottom right panel) The corresponding data at $\mu = 600$ mM. The good agreement between $k^{obs,25\ °C}$ and $k_u^{extrapolated}$ at low pH values shows the accuracy of the extrapolation procedure. The bottom panels show also the unfolding rate constant at pH 6.3 obtained by urea extrapolation k_u^{urea}.

Characterization of the Transition State for Unfolding

(2) pH Dependence of the Interaction Energy of Asp93 in ‡ as Determined by Its Φ value. The Φ value for a particular residue is defined as the extent of interaction between the residue and the rest of the protein (Fersht *et al.*, 1992). For convenience, the Φ value is normalized to $\Phi = 1$ in the native protein where the interaction is defined as fully established and to $\Phi = 0$ in the unfolded state where all interactions with other residues are fully broken. Consequently, the Φ value will increase from 0 to 1 in the course of the refolding process as the interaction consolidates. In a series of earlier studies on barnase, the Φ values for a large selection of residues have been used as structural probes to determine thermodynamically the extent of structure (interactions) in transiently populated conformations like the transition state and the folding intermediate (Matouschek *et al.*, 1989, 1990; Fersht, 1995). The Φ values are determined by relative changes in stability of conformations in the folding pathway upon mutation of the target residues; the Φ value of Asp93 in the transition state is given by

$$\Phi_{\ddagger}^{D93} = 1 - \Delta\Delta G_{\ddagger-N}^{D93N}/\Delta\Delta G_{D-N}^{D93N} \qquad (7)$$

where $\Delta\Delta G_{\ddagger-N}^{D93N}$ is the change in free energy between the transition state and the native state upon mutation of Asp93 to Asn and $\Delta\Delta G_{D-N}^{D93N}$ is the corresponding change between the denatured state and the native state, i.e., the change in stability upon mutation. For a more extensive description of the Φ value approach, see for example Fersht *et al.* (1992) and Fersht, (1995). $\Delta\Delta G_{\ddagger-N}^{D93N}$ is determined from the change in unfolding rate constant upon mutation of Asp93 to Asn, i.e., $\log k_u^{WT} - \log k_u^{D93N}$ (eq 1). The value of $\Delta\Delta G_{D-N}^{D93N}$ has been determined previously in Oliveberg *et al.* (1995a), and its pH dependence is shown together with that of $\Delta\Delta G_{\ddagger-N}^{D93N}$ in the top panel of Figure 6. The Φ value for Asp93 in the transition state for unfolding is calculated according to eq 7 and is plotted versus pH in the bottom panel of Figure 6. At $\mu = 50$ mM, $\Phi_{\ddagger}^{Asp93}$ is about 0.8 between pH 6.3 and 3, the value of $\Phi_{\ddagger}^{Asp93}$ decreases below pH 3, and $\Phi_{\ddagger}^{Asp93} \approx 0.6$ at pH 1.6 (the lowest pH value at which stability data can be obtained for the mutant protein) (Oliveberg *et al.*, 1995a). At $\mu = 600$ mM, $\Phi_{\ddagger}^{Asp93}$ is about 0.7 between pH 6.3 and 3. Below pH 3, the value of $\Phi_{\ddagger}^{Asp93}$ decreases more rapidly than observed at low ionic strengths, and at pH 1.7, $\Phi_{\ddagger}^{Asp93} = 0$ (Figure 6). Between pH 1.7 and 1.0, $\Delta\Delta G_{D-N}^{D93N}$ is approximately 0 and, hence, the Φ value cannot be obtained according to eq 6. At very low pH values, however, $\Phi_{\ddagger}^{Asp93}$ appears to converge at a value similar to that observed above pH 3 (∼0.7).

Characterization of the Folding Pathway

The Asp93 → Asn Mutation Refolds without the Accumulation of a Transient Intermediate. For a two-state process (D ⇄ N), the forward and backward rate constants

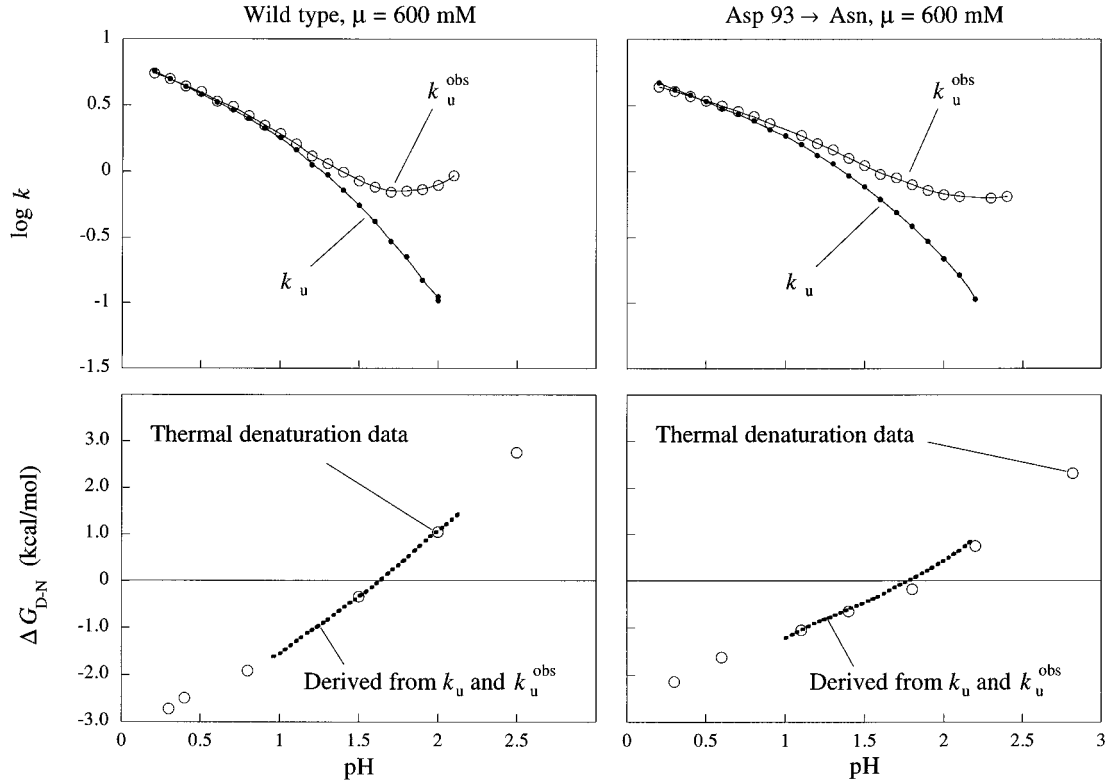

FIGURE 4: Deviation between the observed unfolding rate constant at 25 °C and that extrapolated from 35 °C yields precisely the pH dependence of the protein stability. (Top left panel) Wild-type barnase at $\mu = 600$ mM: (○) the unfolding rate constant observed at 25 °C (k_u^{obs}) and (●) the unfolding rate constant observed at 35 °C and extrapolated to 25 °C ($k_u = k_u^{extrapolated}$). k_u^{obs} and k_u show different values because k_u^{obs} contains components of the refolding rate constant ($k_u^{obs} = k_f + k_u$), whereas the extrapolated data represent the unfolding rate constant only, k_u. (Top right panel) The corresponding data for the Asp93 → Asn mutant. (Bottom left panel) Wild-type barnase at $\mu = 600$ mM. The free energy of unfolding calculated from the deviation between k_u^{obs} and k_u according to eq 6 (dotted line), in comparison with the stability obtained from thermal unfolding experiments (○). (Bottom right panel) The corresponding data for the Asp93 → Asn mutant. The precise agreement between the stability derived from the unfolding kinetics and that obtained from thermal unfolding experiments confirms the validity of the thermal extrapolation method in Figures 3 and 4.

are related to the equilibrium constant according to

$$K_{D-N} = \frac{k_{N\rightarrow D}}{k_{D\rightarrow N}} = \frac{k_u}{k_f} \qquad (8)$$

where K_{D-N} is the equilibrium constant between the native and the denatured protein, $k_{D\rightarrow N} = k_f$ is the refolding rate constant, and $k_{D\rightarrow N} = k_u$ is the unfolding rate constant. With wild-type barnase at pH 6.3, the observed refolding constant (k_f^{obs}) is much lower than that calculated from eq 8 using experimental values of K_{D-N} and k_u (Figure 7). As a plausible explanation, it has been put forward that barnase under these conditions refolds via a folding intermediate and that the (too low) observed refolding rate constant reflects the difference in free energy between the folding intermediate (I) and the denatured state (Scheme 1) (Matouschek *et al.*, 1990).

Scheme 1

$$D \rightleftarrows I \rightleftarrows N$$

Under destabilizing conditions, however, where the folding intermediate becomes less stable than the denatured state, the observed refolding rate constant becomes equal to that calculated from eq 8 (Figure 7). In contrast, the Asp93 → Asn mutant displays two-state behavior under all conditions at $\mu = 600$ mM and only marginal deviations from two-state behavior at $\mu = 50$ mM (Figure 7). Following Scheme 1, the immediate explanation is that deletion of the Asp93−Arg69 salt bridge destabilizes the folding intermediate to such an extent that it does not accumulate in the pre-equilibrium of the refolding process. This suggests that the salt bridge is formed early in the folding pathway and that the ionic interaction between Asp93 and Arg69 contributes significantly to the stability of the folding intermediate.

DISCUSSION

The energetics of the ionic interaction between Asp93 and Arg69 in barnase has been investigated by using mutant proteins in a previous study, and the pK_a value of Asp93 in the native state is estimated to be 0.7 at $\mu = 50$ mM and 1.4 at $\mu = 600$ mM (Oliveberg *et al.*, 1995a). In this study, we extend the investigation of the Asp93−Arg69 salt bridge by focusing on its titration properties and interaction energy in the transition state of unfolding. The Asp93−Arg69 salt bridge is well-suited for mutational studies since it can be considered electrostatically isolated; i.e., it does not interact significantly with other charged residues in the protein. The nearest charged residues are Lys101 and the C-terminus at a distance of approximately 9 and 10 Å, respectively, and so the titration properties of carboxylate groups other than Asp93 are affected only minimally upon mutation of Asp93 to Asn. Hence, changes in the pH dependence of the stability of the mutant protein can be attributed directly to the titration properties of Asp93, and any indirect effects of pK_a shifts of other titrating residues can be neglected. The preliminary

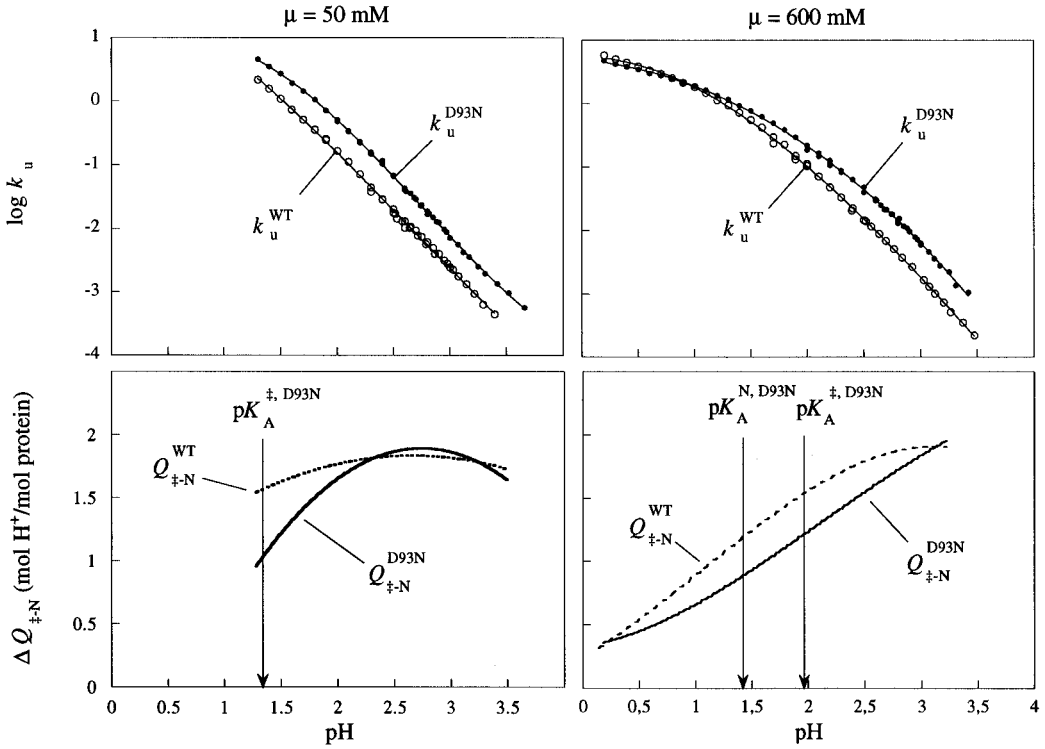

FIGURE 5: pH dependence of the unfolding rate constant related to the protonation difference between the native state and the transition state for wild-type barnase and the Asp93 → Asn mutant. k has units of s^{-1}. (Top left panel) $\mu = 50$ mM: (○) the unfolding rate constant for wild-type barnase (k_u^{WT}) and (●) the unfolding rate constant for the Asp93 → Asn mutant (k_u^{D93N}). (Top right panel) The corresponding rate constants at $\mu = 600$ mM. The fitted curves have been used to represent the experimental data in eq 4. (Lower panels) The derivatives of k_u^{WT} and k_u^{D93N} in the top panels. $\Delta Q_{‡-N}^{WT} = -\partial(\log k_u^{WT})/\partial(\text{pH})$ and $\Delta Q_{‡-N}^{D93N} = -\partial(\log k_u^{D93N})/\partial(\text{pH})$ where ΔQ represents the change in ionization (uptake of protons) between the native protein and the transition state for unfolding (eq 4). At $\mu = 50$ mM, the mutant protein shows a smaller proton uptake than wild-type below pH ~2; the resulting difference between $\Delta Q_{‡-N}^{WT}$ and $\Delta Q_{‡-N}^{D93N}$ reflects the titration of Asp93 in the transition state (see Discussion and simulations in Figure 8). At $\mu = 600$ mM, $\Delta Q_{‡-N}^{WT}$ and $\Delta Q_{‡-N}^{D93N}$ show similar values above pH 3 and below pH 0.3, but $\Delta Q_{‡-N}^{WT} > \Delta Q_{‡-N}^{D93N}$ between these pH values; the difference is related to the titration of Asp93 in the transition state and in the native state (see Discussion and simulations in Figure 8). The arrows indicate the pK_a values of Asp93 in the native protein ($pK_a^{N,Asp93}$) and the pK_a values of Asp93 in the transition state for unfolding ($pK_a^{‡,Asp93}$). $pK_a^{N,Asp93}$ is obtained from Oliveberg *et al.* (1995a), and $pK_a^{‡,Asp93}$ is estimated from the pH dependence of the Φ value of Asp93 in the transition state (see text and Figure 6).

crystal structure of the Asp93 → Asn mutant shows no significant rearrangements of Arg69 or its surrounding residues, which would otherwise have complicated the energetic analysis in this and in the accompanying paper (Pia Harryson, Ashley M. Buckle, and A. R. Fersht, unpublished results).

pK_a Value of Asp93 in the Transition State As Determined by the pH Dependence of the Unfolding Kinetics. An ionizable residue, in this case Asp93, will contribute to $\Delta Q_{‡-N}$, the difference in the number of protons bound to the native state and the transition state, only under conditions where its ionization state in the native protein is different from that in the transition state. Upon mutation of the carboxylate, its contribution to $\Delta Q_{‡-N}$ disappears, and the resulting change in $\Delta Q_{‡-N}$ describes directly the titration of Asp93. We illustrate this by considering the following three scenarios [cf. Discussion in Oliveberg *et al.* (1994)]. (1) At pH values where Asp93 is ionized in both the transition state and the native protein (the ground state), the Asp93 → Asn mutation (D93N) will delete one charge in both conformations and, hence, not affect $\Delta Q_{‡-N}$. (2) At lower pH values, where Asp93 is protonated in the transition state but remains ionized in the native protein, the mutation will delete one charge in the native state but none in the transition state and, therefore, reduces $\Delta Q_{‡-N}$ by 1 unit. (3) At very low pH values, where Asp93 is fully protonated in both the transition state and the native protein, the mutation will not affect the charge difference between the two conformations, and hence, it will not change $\Delta Q_{‡-N}$. Accordingly, an increase in the difference between $\Delta Q_{‡-N}$ for wild-type and mutant protein ($\Delta\Delta Q_{‡-N} = \Delta Q_{‡-N}^{WT} - \Delta Q_{‡-N}^{D93N}$) corresponds to the titration of Asp93 in the transition state and a decrease to its titration in the native state. By inspection of the experimentally observed values of $\Delta Q_{‡-N}$ (Figure 5), it may, thus, be concluded that the pK_a value of Asp93 in the transition state ($pK_a^{‡,Asp93}$) is around 1.3 at $\mu = 50$ mM and around 2.0 at $\mu = 600$ mM (the pK_a values are approximated to be 1 pH unit below the point where $\Delta Q_{‡-N}^{WT}$ and $\Delta Q_{‡-N}^{D93N}$ diverge). The corresponding estimate of the pK_a value of Asp93 in the native state ($\mu = 600$ mM) is 1.3 (Figure 5), which is in good agreement with the result from equilibrium data of 1.4 (Oliveberg *et al.*, 1995a). It can be noticed further in Figure 5 that the maximum value of $\Delta Q_{‡-N}^{WT} - \Delta Q_{‡-N}^{D93N}$ is less than 1. This is so because the pK_a change between the native state and the transition state is relatively small, about 0.5 unit, so that Asp93 starts to titrate in the native state before it is fully protonated in the transition state (cf. simulations in Figure 8).

The Φ Value Analysis and the pH Dependence of the Unfolding Rate Constant Give Consistent Results. $pK_a^{‡,Asp93}$ can also be determined by the pH dependence of

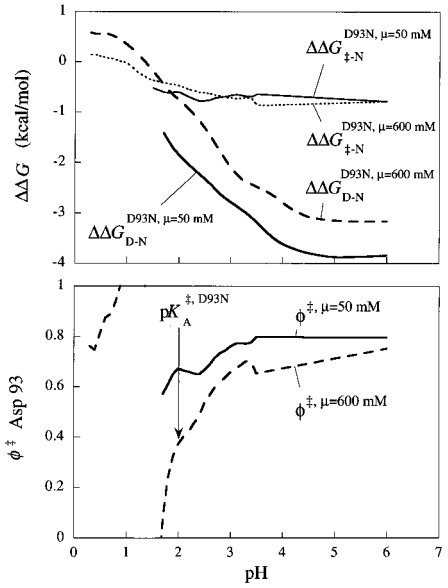

FIGURE 6: Transition state Φ value ($\Phi^{\ddagger}$) for the Asp93 → Asn mutation as a function of pH. $\Phi^{\ddagger}$ represents the extent of interaction of the Asp93 carboxylate group in the transition state relative to its interaction in the native state. (Top panel) The free energy differences in this panel are used to calculate $\Phi^{\ddagger}$ in the bottom panel according to eq 7. The stability change upon mutation of Asp93 to Asn at $\mu = 50$ mM ($\Delta\Delta G_{D-N}^{D93N,\mu=50\ mM}$, thick solid line) and $\mu = 600$ mM ($\Delta\Delta G_{D-N}^{D93N,\mu=600\ mM}$, thick dashed line). The change in activation energy for the unfolding reaction upon mutation of Asp93 to Asn at $\mu = 50$ mM ($\Delta\Delta G_{\ddagger-N}^{D93N,\mu=50\ mM}$, thick solid line) $\mu = 600$ mM ($\Delta\Delta G_{\ddagger-N}^{D93N,\mu=600\ mM}$). (Bottom panel) The pH dependence of $\Phi^{\ddagger}$ at $\mu = 50$ mM (solid line) and $\mu = 600$ mM (dashed line). The pH value at which $\Phi^{\ddagger}$ is reduced by 50% corresponds to the pK_a value of Asp93 in the transition state ($pK_a^{\ddagger,Asp93}$); at this pH, the salt link is fully maintained in the native protein but half-protonated in the transition state.

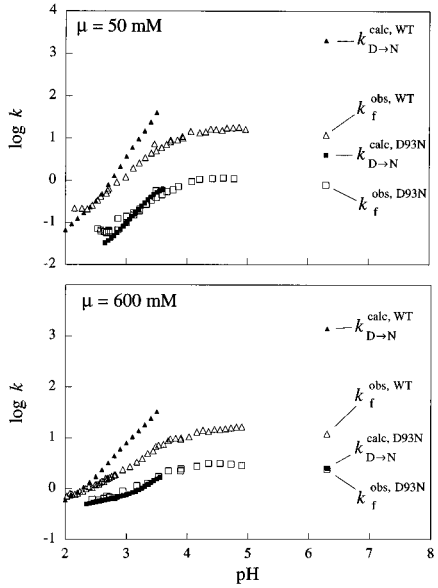

FIGURE 7: Deviation from two-state folding behavior as determined from the deviation between the observed refolding rate constant (k_f^{obs}) and that predicted from a two-state model ($k_{D\rightarrow N}^{calc}$) (eq 8). k has units of s^{-1}. The top panel shows data obtained at $\mu = 50$ mM and the bottom panel data obtained at $\mu = 600$ mM: (△) the observed refolding rate constant for the wild-type protein; $k_f^{obs,WT}$, (□) the observed refolding rate constant for the Asp93 → Asn mutant, $k_f^{obs,D93N}$; (▲) the predicted refolding rate constant for the wild-type protein, $k_{D\rightarrow N}^{calc,WT}$; and (■) the predicted refolding rate constant for the Asp93 → Asn mutant, $k_{D\rightarrow N}^{calc,D93N}$. Whereas wild-type barnase displays a pronounced deviation from two-state behavior, the Asp93 → Asn mutant appears to refold in a two-state process without significant accumulation of a folding intermediate. This observation suggests that the Asp93−Arg69 salt bridge forms early in the folding process and that deletion of this salt bridge destabilizes significantly the components of the pre-equilibrium.

its Φ value. It can be seen in Figure 6 that the Φ value of Asp93 in the transition state decreases rapidly below pH 3. Following earlier investigations (Fersht *et al.*, 1992; Tissot *et al.*, 1996), this decrease can be attributed to a loss of interaction energy of Asp93 in the transition state. In this case, the decreasing Φ value is most likely associated with the titration of Asp93 in the transition state; as the carboxylate group becomes protonated, the ionic interaction with Arg69 is broken. For the Φ value to change, however, the interaction between Asp93 and Arg69 must still be substantially retained in the native (ground) state. By this method, $pK_a^{\ddagger,Asp93} \approx 2.0$ at $\mu = 600$ mM, i.e., the pH where the Φ value has dropped to half its initial value (Figure 6), which is in good agreement with the value determined from $\Delta Q_{\ddagger-N}^{WT} - \Delta Q_{\ddagger-N}^{D93N}$ (Figure 5). The same may be said about the low-salt data if the Φ value is extrapolated *ad hoc* down to pH 1 (Figure 5).

Yet another way to estimate $pK_a^{\ddagger,Asp93}$ experimentally is based on the weakening of the salt link in the transition state. First, the pK_a shift of Asp93 upon refolding of the denatured state is assumed to be directly proportional to the interaction energy of the Asp93−Arg69 salt link. It can be noticed that this simplification assumes that the desolvation component of the pK_a shift is negligible [cf. Bashford and Karplus (1990) and Tissot *et al*. (1996)]. At $\mu = 600$ mM, the pK_a shift of Asp93 in the native state is $4 - 1.4 = 2.6$ (the model compound value minus $pK_a^{N,Asp93}$). Then this pK_a shift of the native state is multiplied by the Φ value of Asp93 at pH 6.3 (Figure 6) to derive the pK_a shift of Asp93 in the transition state, $2.6 \times 0.75 = 1.95$. Finally, $pK_a^{\ddagger,Asp93}$ is obtained by subtracting the transition state pK_a shift from the model compound pK_a value of Asp, $pK_a^{\ddagger,Asp93} = 4 - 1.95 = 2.05$, which is consistent with the two other estimations above. At $\mu = 50$ mM, the corresponding value of $pK_a^{\ddagger,Asp93}$ is $4 - (4 - 0.7) \times 0.8 = 1.36$. Also, this value appears to be consistent with the estimates above. It may be argued, however, that the pK_a value of Asp93 in the denatured state is significantly lower than 4 at low concentrations of salt and that this will result in too high an estimate of $pK_a^{\ddagger,Asp93}$ at $\mu = 50$ mM (Oliveberg *et al.*, 1994, 1995a).

However, the errors associated with the estimations of $pK_a^{\ddagger,Asp93}$ are relatively small, and it appears that interaction energies derived from the pH dependence of the unfolding kinetics and the Φ value analysis give a consistent result. The observation suggests that any structural reorganization of the transition state is insignificant here upon mutation of Asp to Asn.

The Transient Titration Behavior of Ionizable Residues May Reveal Information about the Extent of Conformational Heterogeneity in the Protein-Folding Transition State. When kinetic data are being interpreted, it is essential to know whether the transition state is a single, homogeneous conformation or if the folding reaction proceeds by parallel pathways, i.e., if the kinetics parameters represent a weighted average of several transition states (Baldwin, 1994). To test

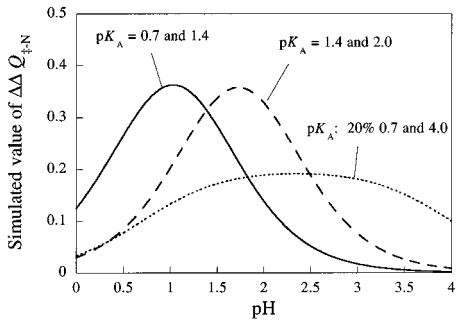

FIGURE 8: Simulations of $\Delta\Delta Q_{‡-N} = \Delta Q_{‡-N}^{WT} - -\Delta Q_{‡-N}^{D93N}$ which examine possible effects of having single or parallel unfolding pathways. In the case of a single pathway, the fractional $\Phi^{‡}$ value of 0.8 is assumed to represent a homogeneous weakening of 20% of the Asp93−Arg69 salt link in the transition state. The pK_a value of Asp93 is then expected to increase in the transition state because of the weakened interaction with Arg69. To simulate $\Delta\Delta Q_{‡-N}$, the pK_a value of Asp93 is set to 0.7 in N and 1.4 in ‡ at $\mu = 50$ mM (solid line) and to 1.4 in N and 2.0 in ‡ at $\mu = 600$ mM (broken line). In the case of parallel pathways, $\Phi^{‡} = 0.8$ is assumed to reflect 20% of the protein unfolding via a transition state in which the salt link is fully broken and 80% of the protein unfolding via a transition barrier in which the salt link remains fully formed. The pK_a value of Asp93 in the fully broken pathway is set to the model compound value of about 4, and the pK_a value of Asp93 in the predominant fully formed pathway is set to the pK_a value of the native protein, 0.7 (dotted line). Comparison of the various simulations of $\Delta\Delta Q_{‡-N}$ with experimental observations of $\Delta Q_{‡-N}^{WT}$ and $\Delta Q_{‡-N}^{D93N}$ (Figure 5) favors the interpretation of a single pathway.

the possibility of multiple pathways, we have adopted the following strategy. As a minimal model, the folding reaction is assumed to proceed by any of three mechanisms. (1) The first is a single uniformly expanded transition state. The Φ value represents in this simple case the homogeneous weakening of a specific interaction. (2) The second is a statistical distribution of interconverting transition states in which each conformation represents a unique set of either fully formed or fully broken interaction units. The average of all these conformations may still be treated as a single transition state, although the folding reaction in fact proceeds by a diffuse ensemble of parallel pathways. The Φ value then represents the statistical average of fully formed and fully broken interactions of a specific target residue. (3) The third is two or more clearly distinct transition states that do not interconvert. In this case, the Φ value corresponds to the weighted average of a specific interaction in two or more parallel pathways.

With a uniformly expanded transition state, the weakening of a salt link results in a uniform pK_a shift of the carboxylate group. The shift gives rise to a single pK_a value which is the same in the whole population of identical transition states. To be consistent with earlier work on barnase, the general interpretation of data in this study is based on this (minimal) model, and simulations of effects on $\Delta Q_{‡-N}$ are shown in Figure 8. The results from the simulations, based on the pK_a values determined above, are in reasonable agreement with the experimental observations in Figure 5; i.e., the results are consistent with the transition state being a uniformly expanded species [cf. Matthews and Fersht (1995)].

Although it is difficult to derive a mathematical model for a statistical distribution of interconverting transition states, it is likely that such a mechanism will result in a behavior similar to that of the uniformly expanded transition state. At present, we know no means of distinguishing between mechanism 1 and 2.

The predictions from a simplified parallel pathway mechanism turn out somewhat different. In order to rationalize the simulation, only two pathways were considered: one in which the Asp93−Arg69 salt bridge is fully formed and one in which the interaction is fully broken. On the basis of the Φ value of Asp93, 80% of the protein molecules was assumed to follow the "fully formed" pathway and 20% the "fully broken". Further, the pK_a value of Asp93 in the fully formed transition state was assumed to be similar to that in the native protein so that this pathway does not significantly contribute to $\Delta Q_{‡-N}$. The pK_a value of Asp93 in the fully broken was assumed to be similar to that in the denatured state, i.e., 4. Consequently, the contribution of Asp93 to $\Delta Q_{‡-N}$ will be 20% of a proton between pH ∼4 and ∼1 (Figure 8). This behavior, however, appears less consistent with the results in Figure 5 than are models 1 and 2.

It must be pointed out that the purpose of the simulations in Figure 8 is not to prove the nature of the transition state of barnase but rather to exemplify how energetics and transient pK_a shifts may be used to obtain information about structural heterogeneity in general; since the properties of transient conformations can only be studied indirectly by kinetic methods, it is crucial to develop and to test a wide range of independent approaches.

Role of Salt Bridges in Early Folding Events. In contrast to the behavior wild-type barnase, the folding behavior of the Asp93 → Asn mutant resembles that of a two-state process (Scheme 1, Figure 7). This indicates that any folding intermediate is substantially destabilized by the mutation of Asp93 so that the denatured state constitutes the most populated conformation in the pre-equilibrium D ⇄ I (cf. Scheme 1). Since the observed refolding rate constant in this case represents mainly the free energy difference between the denatured state and the transition state, it is impossible to derive exact information about the energetics of any other conformations in the pre-equilibrium [see discussion about pre-equilibrium effects in Oliveberg and Fersht (1996a)]. Following the three-state model in Scheme 1, however, it may still be concluded that the interaction energy of Asp93 in the folding intermediate at least matches the overall stability of this conformation, i.e., 2−3 kcal/mol. In other words, the Asp93−Arg69 salt bridge appears to be formed in the very initial events of the folding process. This suggests that the formation of ionic interactions plays a part in the early condensation of the disordered polypeptide chain. In fact, charge−charge interactions are effective over longer atomic distances than are the predominant van der Waals contacts. Hence, salt links may form more rapidly in a disordered polypeptide and steer the overall consolidation of short-distance hydrophobic interactions. Once the positive and negative charges are paired in a hydrophobic environment, the activation barrier for dislocating the salt link is high; the dislocation process will involve isolated charges in a hydrophobic environment which is highly unfavorable energetically. Accordingly, a buried salt link could kinetically direct the folding pathway even if it does not stabilize the structure *per se*. The idea is in line with previous reports on native structures which suggest that the role of buried salt bridges is not energetic but perhaps to add structural specificity to the native conformation (Jencks, 1969; Fersht

et al., 1985; Hendsch & Tidor, 1994; Tissot *et al.*, 1996; Waldburger *et al.*, 1995). The concept may here be taken one step further; the role of salt bridges is not to stabilize the protein thermodynamically but to add specificity early in the folding process and to control the folding pathway kinetically.

Observations of the folding intermediate of barnase suggest that this is a significantly structured and dehydrated conformation at pH 6.3 (Matouschek *et al.*, 1992; Oliveberg & Fersht, 1996b); at lower pH values, however, where kinetic and thermodynamic data predict the intermediate to be populated under equilibrium conditions, the structural content of the denatured species appears low (Arcus *et al.*, 1994). An explanation for this apparent inconsistency could be that at pH 6.3 the folding intermediate is kept in a unique structural conformation by internal ion pairs, whereas at low pH, the carboxylate group in these salt links becomes protonated and the structure of the intermediate rearranges to solvate better the remaining positively charged amino group. Along these lines, it is tempting to speculate that protonated and rearranged folding intermediates which have lost part of their structural specificity constitute the so-called molten-globule conformations (Ptitsyn, 1992; Oliveberg & Fersht, 1996b).

REFERENCES

Arcus, V., Vuilleumier, S., Freund, S. M. V., Bycroft, M., & Fersht, A. R. (1994) *Proc. Natl. Acad. Sci. U.S.A. 91*, 9412−9416.

Arrhenius, S. (1889) *Z. Phys. Chem. 4*, 226−248.

Baldwin, R. L. (1994) *Nature 369*, 183−184.

Bashford, D., & Karplus, M. (1990) *Biochemistry 29*, 10219−10225.

Buckle, A. M., Henrick, K., & Fersht, A. R. (1993) *J. Mol. Biol. 234*, 847−860.

Chen, B., Baase, W. A., & Schellman, J. A. (1989) *Biochemistry 28*, 691−699.

Eriksson, A. E., Baase, W. A., Zhang, X. J., Heinz, D. W., Blaber, M., Baldwin, E. P., & Matthews, B. W. (1992) *Science 255*, 178−183.

Eyring, H. (1935) *Chem. Rev. 35*, 65−77.

Fersht, A. R. (1993) *FEBS Lett. 325*, 5−16.

Fersht, A. R. (1995) *Curr. Opin. Struct. Biol. 5*, 79−84.

Fersht, A. R., Shi, J. P., Knill-Jones, J., Lowe, D. M., Wilkinson, A. J., Blow, D. M., Brick, P., Carter, P., Waye, M. M. Y., & Winter, G. (1985) *Nature 314*, 235−238.

Fersht, A. R., Matouschek, A., & Serrano, L. (1992) *J. Mol. Biol. 224*, 771−782.

Hendsch, Z. S., & Tidor, B. (1994) *Protein Sci. 3*, 211−226.

Itzhaki, L. S., Daniel, E. O., & Fersht, A. R. (1995) *J. Mol. Biol. 254*.

Jackson, S. E., & Fersht, A. R. (1991) *Biochemistry 30*, 10428−10435.

Jackson, S. E., Moracci, M., el Masry, N., Johnson, C. M., & Fersht, A. R. (1993) *Biochemistry 32*, 11259−11269.

Jencks, W. P. (1969) *Catalysis in Chemistry and Enzymology*, McGraw-Hill Inc., New York.

Matouschek, A., Kellis, J. T., Jr., Serrano, L., & Fersht, A. R. (1989) *Nature 342*, 122−126.

Matouschek, A., Kellis, J. T., Jr., Serrano, L., Bycroft, M., & Fersht, A. R. (1990) *Nature 346*, 440−445.

Matouschek, A., Serrano, L., & Fersht, A. R. (1992) *J. Mol. Biol. 224*, 819−835.

Matthews, J. M., & Fersht, A. R. (1995) *Biochemistry 34*, 6805−6814.

Oliveberg, M., & Fersht, A. R. (1996a) *Biochemistry 35*, 2726−2737.

Oliveberg, M., & Fersht, A. R. (1996b) *Biochemistry 35*, 2738−2749.

Oliveberg, M., Vuilleumier, S., & Fersht, A. R. (1994) *Biochemistry 33*, 8826−8832.

Oliveberg, M., Arcus, V., & Fersht, A. R. (1995a) *Biochemistry 34*, 9424−9433.

Oliveberg, M., Tan, Y. J., & Fersht, A. R. (1995b) *Proc. Natl. Acad. Sci. U.S.A. 92*, 8926.

Otzen, D. E., Itzhaki, L. S., ElMasry, N. F., Jackson, S. E., & Fersht, A. R. (1994) *Proc. Natl. Acad. Sci. U.S.A. 91*, 10422−10425.

Pohl, F. M. (1976) *FEBS Lett. 65*, 293−296.

Ptitsyn, O. B. (1992) in *Protein Folding* (Creighton, T. E., Ed.) W. H. Freeman and Co., New York.

Sayers, J. R., Schmidt, W., & Eckstein, F. (1988) *Nucleic. Acids Res. 16*, 791−802.

Serrano, L., & Fersht, A. R. (1989) *Nature 342*, 296−299.

Serrano, L., Matouschek, A., & Fersht, A. R. (1992) *J. Mol. Biol. 224*, 805−818.

Sugihara, M., & Segawa, S. (1984) *Biopolymers 23*, 2473.

Tanford, C. (1970) *Adv. Protein Chem. 24*, 1−95.

Tissot, A., Vuilleumier, S., & Fersht, A. R. (1996) *Biochemistry 35*, 6786−6794.

Waldburger, C. D., Schildbach, J. F., & Sauer, R. T. (1995) *Struct. Biol. 2*, 122−128.

BI9529317